Biochemical and Biophysical Research Communications 446 (2014) 218–223

Contents lists available at ScienceDirect

Biochemical and Biophysical Research Communications

journal homepage: www.elsevier.com/locate/ybbrc

Detection of PIWI and piRNAs in the mitochondria of mammalian cancer cells

ChangHyuk Kwon [a], Hyosun Tak [b], Mina Rho [c], Hae Ryung Chang [d], Yon Hui Kim [d], Kyung Tae Kim [e], Curt Balch [f], Eun Kyung Lee [b], Seungyoon Nam [a,*]

[a] Cancer Genomics Branch, National Cancer Center, Goyang 410-769, Republic of Korea
[b] Department of Biochemistry, College of Medicine, Catholic University of Korea, Seoul 137-701, Republic of Korea
[c] Department of Computer Science, Hanyang University, Seoul 133-791, Republic of Korea
[d] New Experimental Therapeutics Branch, National Cancer Center, Goyang 410-769, Republic of Korea
[e] Molecular Epidemiology Branch, National Cancer Center, Goyang 410-769, Republic of Korea
[f] Medical Sciences Program, Department of Cellular & Integrative Physiology, Indiana University School of Medicine, Bloomington, IN 47405, USA

ARTICLE INFO

Article history:
Received 12 February 2014
Available online 3 March 2014

Keywords:
Small RNA-Seq
Bioinformatics
Genomics
Sequence analysis
piRNA
Piwi
Mitochondria
Non-coding RNAs

ABSTRACT

Piwi-interacting RNAs (piRNAs) are 26–31 nt small noncoding RNAs that are processed from their longer precursor transcripts by Piwi proteins. Localization of Piwi and piRNA has been reported mostly in nucleus and cytoplasm of higher eukaryotes germ-line cells, where it is believed that known piRNA sequences are located in repeat regions of nuclear genome in germ-line cells. However, localization of PIWI and piRNA in mammalian somatic cell mitochondria yet remains largely unknown. We identified 29 piRNA sequence alignments from various regions of the human mitochondrial genome. Twelve out 29 piRNA sequences matched stem-loop fragment sequences of seven distinct tRNAs. We observed their actual expression in mitochondria subcellular fractions by inspecting mitochondrial-specific small RNA-Seq datasets. Of interest, the majority of the 29 piRNAs overlapped with multiple longer transcripts (expressed sequence tags) that are unique to the human mitochondrial genome. The presence of mature piRNAs in mitochondria was detected by qRT-PCR of mitochondrial subcellular RNAs. Further validation showed detection of Piwi by colocalization using anti-Piwil1 and mitochondria organelle-specific protein antibodies.

1. Introduction

Piwi family proteins and their cognate small non-coding RNAs (Piwi-interacting RNAs, piRNAs), are essential for the differentiation of male primordial germ cells [1,2]. It is believed that they protect the genome by facilitating transcriptional and post-transcriptional silencing of transposable elements via heterochromatization and endonucleolytic cleavage, respectively [3–5].

The piRNAs are small noncoding RNAs of 26–31 nucleotides in length, and are generally processed from their longer precursors that are transcribed from repetitive elements, introns and 3′UTR regions [1]. During processing, Piwi family proteins are involved in cleavage of the longer piRNA precursors [1,2].

Consistent with their association with piRNAs, Piwi family proteins, generally localized in the cytosol and nucleus, are associated with DNA methylation, transposon repression, and translational repression, in germ line cells and somatic follicular cells of the *Drosophila* ovary [5,6]. Piwi family proteins and piRNAs have also been identified in higher eukaryotes and the mammalian Piwi ortholog has been implicated in infertility and cancer [6–9]. However, despite increased recognition of Piwi and piRNAs in the pathogenic associations, piRNA sequence location and Piwi localization to mitochondria remains largely unknown [10–12].

In this study, we utilized both computational and experimental analyses to study the possible presence of Piwi and piRNA transcripts in mitochondria from human normal and cancer cell lines. Using small RNA-Seq databases, we identified mitochondrial piRNA transcripts which comprise a previously unknown subset of mitochondrial small non-coding RNAs. Considering piRNAs have their longer precursors [1,2], we also discovered multiple long

* Corresponding author. Address: Cancer Genomics Branch, National Cancer Center, 323 Ilsan-ro, Ilsandong-gu, Goyang, Gyeonggi-do 410-769, Republic of Korea. Fax: + 82 31 920 2542.
E-mail addresses: netbuyer@hanmail.net (C. Kwon), chuberry@naver.com (H. Tak), minarho@hanyang.ac.kr (M. Rho), heyhae@ncc.re.kr (H.R. Chang), yhkim@ncc.re.kr (Y.H. Kim), bioktkim@ncc.re.kr (K.T. Kim), curt.balch@gmail.com (C. Balch), leeek@catholic.ac.kr (E.K. Lee), seungyoon.nam@ncc.re.kr (S. Nam).

http://dx.doi.org/10.1016/j.bbrc.2014.02.112
0006-291X/

mitochondria-unique expressed sequence tags (ESTs) that overlapped the piRNA transcripts. Further support for mitochondrial presence of piRNA and Piwi, was provided by qRT-PCR and Western blot in mitochondrial subcellular fractions. To our knowledge, this is the first report on localization of piRNAs and Piwi proteins in mammalian cancer cell mitochondria.

2. Material and methods

2.1. Mapping piRNAs and mitochondrial small RNA-Seq to mtDNA

In order to locate piRNA sequences in mtDNA, we mapped known piRNA sequences [13] to the human mitochondrial genome [GenBank: NC_001807], which was downloaded from UCSC Genome Browser (GB) web site (genome.ucsc.edu). Carmell and colleagues experimentally identified the piRNA sequences [13]. Using those sequences [13] [GenBank: DQ539889 to DQ569912] from NCBI GenBank, we found 29 piRNAs (Fig. 1) that formed perfect matches with the mtDNA genomic sequence by using BLAST (Table S1). Moreover, 12 out of the 29 identified piRNAs also perfectly matched sequence fragments from seven tRNAs (tRNA-Phe, -Val, -Leu, -His, -Ser, -Glu, and -Thr).

We used small RNA-Seq datasets (from mitochondrial subcelluar fractions) to measure read depths of the 29 piRNA regions in mitochondria. Based on the multiple datasets, we inspected the read depths of the piRNAs. The small RNA-Seq dataset of HeLa and HEK293 cells was downloaded from NCBI Gene Expression Omnibus (GEO, ncbi.nlm.nih.gov/geo) under the accession number GSE32185 [10] (see read length distribution in Fig. S1). The small RNA-Seq dataset of 143B cell line was obtained from NCBI GEO under the accession number GSM763531 [12]. We then filtered the small RNA-Seq reads by using FASTQ Groomer (galaxyproject.org) [14], with default options and a minimum Phred quality score of 20. The small RNA-Seq reads of the three cell lines were mapped to the human mitochondrial genome [GenBank: NC_001807] by using the default options of the Burrows–Wheeler Alignment tool (BWA) [15] and SAMtools [16]. Read depths at mitochondrial DNA (mtDNA) genomic positions were obtained using the default options of BEDTools [17], and are visualized in Fig. 2A. To determine the expression of each 5′ and 3′ tRNA fragment (Fig. 2B and Table S2), we calculated the average read depth for each fragment. The expression of the 5′ fragment was measured by the average read depth of the 26 bases in the middle of the tRNA 5′ half region. The expression of the 3′ fragment was measured by the average read depth of the 26 bases in the middle of the tRNA 3′ half region.

2.2. Identification of uniquely mtDNA-mapped expressed sequence tags (ESTs) containing the 29 piRNAs

Since expressed sequence tags (ESTs) contain non-coding RNA fragments and their precursor fragments [18], we reasoned that the longer ESTs around the piRNAs exist as their precursors (or precursor-like transcripts). We further focused on uniqueness of the ESTs in mtDNA (not in nuclear DNA), since the unique alignment indicates the ESTs are soley transcribed from mtDNA. To assess whether unique mitochondrial ESTs contained the 29 piRNA sequences, we used the GenBank EST (ncbi.nlm.nih.gov/dbEST) alignment information table all.est deposited in the UCSC GB [19], extracting unspliced ESTs uniquely mapped to mtDNA (not nuclear DNA). The alignment was made by BLAT [19]. That comparison of the unique ESTs and the piRNAs (using the UCSC GB table browser tool) resulted in our identification of 4494 mitochondria-specific, unspliced ESTs overlapping (or partially overlapping) the 29 piRNA sequences. In addition, tissue- and cell type-specificities of the piRNA-containing ESTs were obtained from table gbCdnaInfo that includes library description information (e.g., cell- and tissue-type), as extracted from the UCSC Genome Browser database [19].

2.3. Western blot analysis

Neuroblastoma Neuro2a cells were fractionated by differential centrifugation, as previously described by Yu et al. [20]. Briefly, after washing with PBS, cells were resuspended in isotonic homogenization buffer (10 mM Tris–HCl (pH 7.4), 250 mM sucrose, 10 mM KCl, 1.5 mM $MgCl_2$, 1 mM EDTA, 1 mM dithiothreitol and protease inhibitor cocktail). After 100 strokes in a Dounce homogenizer, unbroken cells were removed by centrifugation at $30\times g$ for 5 min. The nuclei and mitochondrial fractions were prepared from the resuspended pellets by centrifugation at $80\times g$ for 10 min and $6000\times g$ for 20 min, respectively. The final supernatant was used as the cytosolic fraction.

For Western blot analysis, protein samples were separated by SDS–PAGE, transferred to PVDF membranes, and incubated with primary antibodies against Lamin-B (Abcam), Piwi (Abcam; ab12337 (Anti-PIWIL1 antibody)), β-actin (Abcam), and Tom40 (Santa Cruz Biotech, a mitochondrial marker) antibodies. Following incubation with HRP-conjugated secondary antibodies, immunoluminescence was determined using ECL Prime kits (GE Healthcare). Thus, we used Lamin-B, Tom40, and α-tubulin antibodies as nuclear, mitochondrial, and cytosolic markers, respectively, to examine possible colocalization with Piwi. β-actin was used as a loading control.

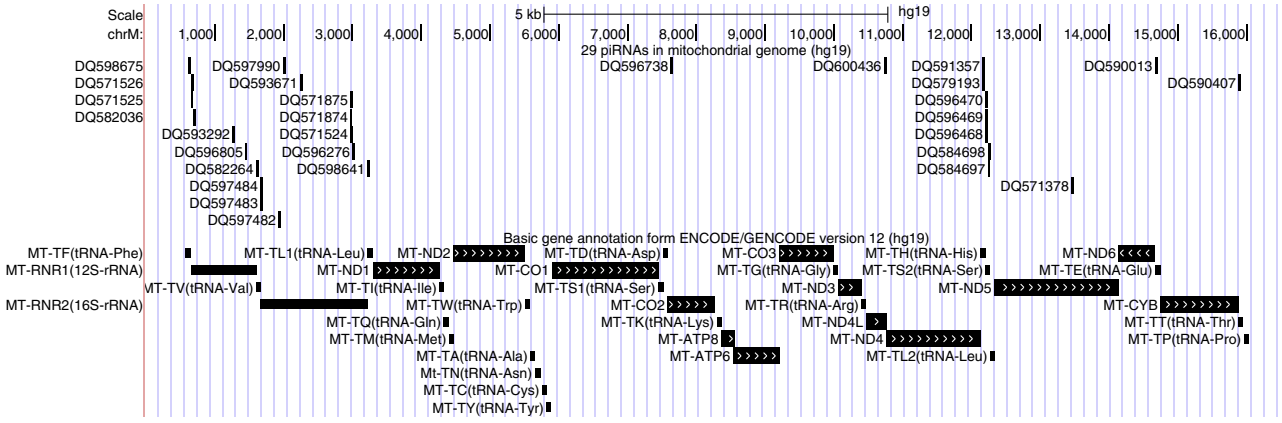

Fig. 1. Mitochondrial genomic location of the 29 piRNAs. The panel has two tracks: the 29-piRNAs (upper track) and mtDNA annotations (lower track). The piRNAs are located throughout mitochondrial genome, including rRNA regions, tRNA regions, and protein-coding regions.

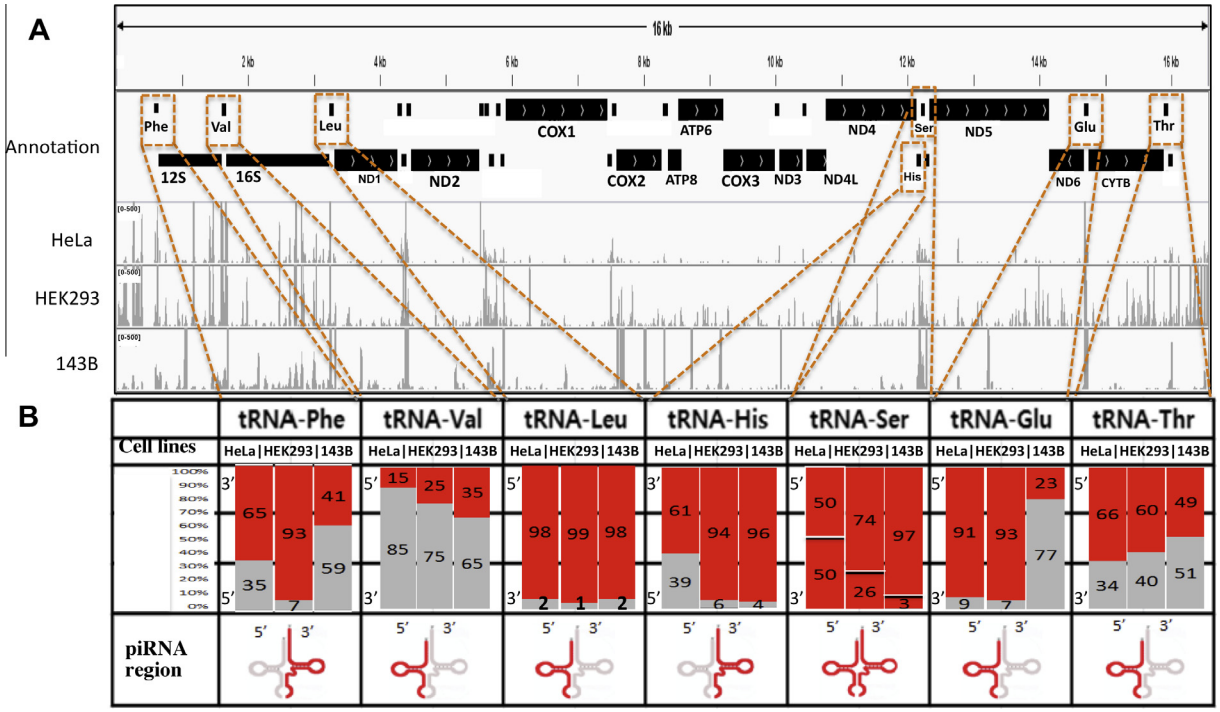

Fig. 2. Distribution of small RNA reads of mitochondrial subcellular fractions from HeLa, HEK293, and 143B cells. (A) This panel consists of four tracks: mtDNA gene annotation (including tRNA, rRNA, and protein-coding genes), below which are small RNA-Seq reads from HeLa (top), HEK293 (middle), and143B (bottom) cells. Dashed boxes in orange indicate 7 tRNAs (of mtDNA) encompassing piRNAs. The regions of the piRNAs in the tRNAs are represented in B. (B) At the bottom row of the table, the tRNA subsequence encompassing each piRNA is shown in red. In the third row, the three columns for each tRNA indicate the average read depths of HeLa, HEK293, and 143B cells, respectively. The average depths for the 5′ region and the 3′ region of each tRNA in the three cell lines are presented as bar graphs: red bars indicate expression levels of each specific piRNA-corresponding fragment; gray bars represent the expression of the non-piRNA-corresponding fragments. The percentage represented in bar graph was obtained from the average read depth of the region divided by summation of the average read depths of both 5′ and 3′ regions in the tRNA (Table S2). (For interpretation of the references to color in this figure legend, the reader is referred to the web version of this article.)

2.4. RT-qPCR

HeLa (HeLa-S3) cell total RNA was isolated from whole cells or specific subcellular fractions (*i.e.*, cytosol, mitochondrial, and/or nuclear) using TRIzol reagent (Invitrogen), according to the manufacturer's protocol. cDNA was prepared using the Quanti-Mir RT system (System Bioscience, Inc.) according to the manufacturer's protocol. The abundance of specific transcripts was assessed by quantitative (q)PCR analysis using a SYBR green PCR master mix (Kapa Biosystems). The piRNA-specific primer sequences ([GenBank: DQ590013] (piR-57125), 5′-TGGTCGTGGTTGTAGTCCG TG-3′; [GenBank: DQ598641] (piR-36707), 5′-GTTAAGATGGCAGA GCCCGG-3′; [GenBank: DQ598675] (piR-36741), 5′-GTTTAGAC GGGCTCACATCAC-3′) and universal reverse primer (System Bioscience, Inc.) were used. RT-qPCR analysis was performed with Applied Biosystems 7300 model. The piRNA expression was normalized to the small RNA U1 [21].

3. Results

3.1. Mapping piRNAs and mitochondrial small RNA-Seq to mtDNA

As recent studies have reported the presence of small RNAs in the mitochondria, the possibility that a subset of these could be piRNA species remains. To examine this, we first located perfectly aligned piRNA sequences in mtDNA and subsequently obtained read depths of the mtDNA-mapped piRNAs by aligning small RNA-Seq reads.

As a result, we identified that a total of 29 piRNAs (Table S1) formed perfect matches with the mtDNA genomic sequence [10,12]. Of those 29 piRNAs, 12 mapped to subsequences of the 7 tRNAs (tRNA-Phe, -Val, -Leu, -His, -Ser, -Glu, and -Thr), 14 mapped to subsequences of the 12S and 16S rRNAs, and three mapped to subsequences of the mitochondrial protein-coding genes *COX2*, *ND4L*, and *ND5* (Fig. 1).

We subsequently inspected mitochondrial small RNA-Seq datasets from malignant (HeLa, 143B) and normal (HEK293) human cell lines [10,12], obtained from NCBI GEO (accession number: GSE32185, GSM763531), to determine the expression (*i.e.*, read depths) of the piRNAs in mitochondria. Fig. 2A demonstrated the read depth distributions of mitochondrial small RNA reads from the three cell lines. The seven tRNA regions (depicted in the orange box in Fig. 2A) encompassing the 12 piRNA sequences revealed small RNA reads. Intriguingly, we also observed an asymmetric tRNA fragment usage from their 5′ and 3′ regions, as implicated by differential read mapping (Fig. 2B). We found that HeLa, 143B, and HEK293 cells favored 5′ tRNA fragments over 3′ fragments by factors of 1.4, 1.7, and 2.5, respectively (Table S2). Conversely, in all three cell lines, 3′ fragments of the tRNA-Val and -His were favored over 5′ fragments, while the 3′ fragments of tRNA-Phe in HeLa and HEK293 cells (in contrast to 143B cells) were favored over 5′ fragments (Fig. 2B). Likely asymmetric fragment usage was further illustrated by HeLa and HEK293 tRNA-Glu and -Thr preferences for 5′ fragments, again in contrast to 143B cells (which favored 3′ fragment matches) (Fig. 2B).

We also found piRNA sequences that matched both the 5′ and 3′ fragments of tRNA-Ser (Fig. 2B), suggesting dual-end generation of piRNAs. Out of the seven tRNAs matching the 12 piRNAs, tRNA-Leu associated with a highly expressed (>98%) piRNA, piR-36707 [GenBank: DQ598641] in all the three cell lines (HeLa, HEK293, 143B), while tRNA-His in HEK293 and 143B cells associated with two

highly expressed (>94%) piRNAs, piR-58469 and piR-47305 ([GenBank: DQ591357] and [GenBank: DQ579193], respectively) (Fig. 2B and Table S2). This observation is consistent with cell type-specific activities (or subcellular localizations) of distinct tRNA endoribonucleases and/or RNase inhibitors [22,23] involved in RNA processing. Since the tRNA fragments have common or differential usages in the three cell types, piRNA expression could also be closely correlated with the expression of their precursor transcripts.

3.2. ESTs overlapping with piRNA sequences map uniquely to mtDNA

To identify possible mtDNA-derived precursor transcripts, we inspected the GenBank EST database (ncbi.nlm.nih.gov/dbEST/) and the alignment table [19] of the UCSC Genome Browser (genome.ucsc.edu). We reasoned that since mitochondrial-unique, long ESTs could include non-coding RNA fragments and their precursor fragments [18], these might represent alternative piRNA precursor fragments (besides nuclear DNA). It is important that the unique assignment of the longer ESTs to mtDNA (not nuclear DNA) at least indicates mtDNA-derived transcription of the potential piRNA precursors. Thus, unspliced EST transcripts uniquely mapping to the mitochondrial genome might represent potential mtDNA-encoded precursors of the mitochondrial piRNAs.

As ESTs are generally longer than small RNAs (or tRNAs), we can identify not only mitochondria-unique ESTs, but also their library description information (e.g., cell type, tissue type). As a result, utilizing publicly available GenBank EST sequences aligned by the UCSC GB, we identified 4494 mitochondria-unique ESTs (Fig. 3A, visualized by Integrative Genomics Viewer [24]) overlapping majority of the 29 piRNAs. This result strongly suggests that processing of mitochondrial piRNA precursors into their mature piRNAs occurs within that specific organelle. In other words, the result would imply that some fraction of these 29 piRNAs comes from biogenesis of piRNAs in the mitochondria, as well as results from intracellular translocation of nuclear RNA transcripts into mitochondria.

We further assessed possible tissue specificity of the mitochondrial genome-specific unspliced ESTs overlapping the 29 piRNAs. That analysis demonstrated a global tissue distribution of these ESTs in normal tissues and tumors, including hepatocellular, gastric (GC), kidney, neuroblastoma, cervical, osteosarcoma, prostate, and endometrial cancers (Table S3). Consequently, this result supports both global and cancer-associated, mitochondria-specific (and not nuclear DNA) transcription of potential piRNA precursors.

We also analyzed the library description information of the mtDNA-unique unspliced ESTs in various normal and cancer cell lines, revealing GC, neuroblastoma, and prostate cancer cells to possess the piRNA-associated unspliced ESTs (Table S4). In particular, we also identified nine distinct GC cell lines expressing the unspliced ESTs (Table S4), in agreement with a previous study showing upregulated piRNA expression in GC and other cancer cells [25]. Consequently, our EST analysis suggests that cancer cells differentially transcribe mitochondrial piRNA precursors. Minimally, our analysis suggests that cell/tissue-specific transcription in mitochondria in terms of the precursor-like transcripts associated with the piRNAs (Tables S3 and S4).

3.3. Subcellular distribution of piRNAs and Piwi proteins

To confirm the assignment of three abundant mature piRNA sequences (DQ590013, DQ598641, and DQ598675) to subsequences of mitochondrial tRNAs-Glu, -Leu, and -Phe, we quantified their expression levels by qRT-PCR in HeLa-S3 cells. Those analyses demonstrated that these three mitochondrial piRNAs exist not only in mitochondrial subcellular fractions, but also in the cytoplasm and nucleus (Fig. 3B).

As shown in Fig. 3B, those assessments also demonstrated DQ590013 (piR-57125) and DQ598641 (piR-36707) as predominantly cytosolic, while DQ598675 (piR-36741) was abundant in both the mitochondria and nucleus. These findings suggest that piRNAs, in general, are distributed unevenly throughout various subcellular compartments.

While a mitochondrial presence of Piwi proteins has been shown in murine germ-line cells [11], we are not aware of any reported presence in the mitochondria of mammalian cells, including cancer cells. Since Piwi family proteins are known as cognate binding partners of piRNAs, we thus investigated mitochondrial localization of Piwil1 protein by inspecting its N-terminus for a possible mitochondrial targeting signal (NP_004755), using the prediction tool MitoProt II [26] (ihg.gsf.de/ihg/mitoprot.html). That prediction demonstrated a high probability (79.3%) of mitochondrial localization (Fig. S2).

To confirm that computational result (*i.e.*, high probability of mitochondrial targeting), we performed Western blot analysis. Since neuroblastoma was one specific tumor strongly expressing the mitochondrial piRNA-matched ESTs (Tables S3 and S4), we fractionated Neuro2a cell lysates by differential centrifugation into three subcellular (nuclear, mitochondrial, and cytoplasmic) fractions. The organelle specificity of those differentially obtained fractions was confirmed by immunoblotting with an antibody against the mitochondria-specific protein Tom40, as compared to antibodies against Lamin-B and β-actin, which were found in all three subcellular fractions (including the cytosol and nucleus) [20]. As depicted in Fig. 3C, Piwil1 was detected in both nuclear and mitochondrial fractions, thus supporting our earlier computational prediction of Piwi translocalization to the mitochondrion.

4. Discussion

While the majority of studies on piRNAs and Piwi proteins have focused on transposable repeats in nuclear DNA of germ-line cells, we here detected numerous piRNAs to align with mitochondria-specific small RNA sequencing libraries in cancer cells. Through computational analysis, piRNAs in mitochondria can be transcribed from mtDNA itself, but we should not exclude the possibility of translocation of piRNAs from the nucleus (or cytosol) to mitochondria. Our experimental studies further show co-existence of Piwi protein and its cognate RNAs (piRNAs) in mitochondria, suggesting possible "crosstalk" of Piwi–piRNA pathways between the nucleus and mitochondria.

Based on our findings, we can speculate a possible function(s) of Piwi/piRNAs in the mitochondria. Our findings raise a possibility that mt piRNAs likely derive from mt tRNAs and rRNAs. These mt piRNAs need to be inspected in terms of possible association with stress responses [22,27]. Of interest, in the parasite *Leishmania*, a Piwi analog localizes to its single mitochondrion and may play a role in mitochondria function and resistance to apoptosis [28]. As mitochondria are well known contributors to oxidative stress [22,29], one could postulate mt piRNA and Piwi involvement in mediating cellular behavior related to such stress.

Since cancer cells often benefit from enhanced stress responses [30], it is possible that mitochondrial Piwi and tRNA-generated piRNAs could contribute to cellular injury repair mechanisms. Indeed, we found high expression levels of mt piRNA precursor transcripts in numerous cancer cell types and tumors (Tables S3 and S4), in agreement with a previous study showing elevated piRNA levels in gastric cancer cells [25].

In agreement with our current indication of the presence of neuroblastoma mitochondrial Piwi, it was previously shown that Piwi knockdown in *Drosophila melanogaster* suppressed the growth of malignant brain tumors [31]. Additional support for a

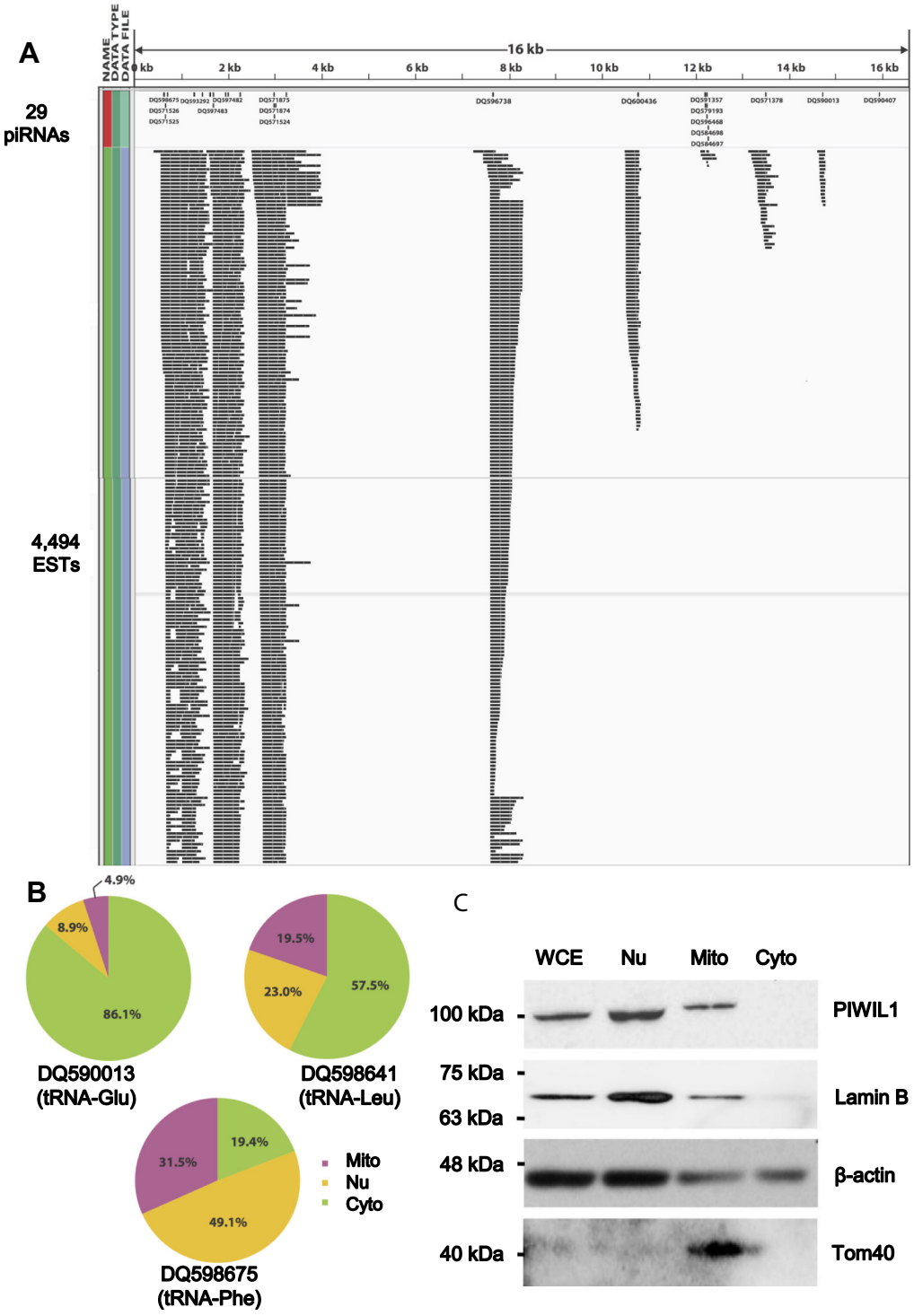

Fig. 3. Presence of piRNA sequences and Piwi in mitochondria. (A) The 4494 mitochondrial-unique unspliced ESTs overlapping the 29 piRNAs. The first track (red horizonal bar) indicates whole human mtDNA. The second track represents the locations of the 29 piRNAs. The last track shows the locations of all the 4,494 ESTs. (B) Expression of the three mtDNA-derived piRNAs (normalized to small RNA U1) in the three subcellular fractions (nucleus, cytosol, and mitochondria) in HeLa-S3. The piRNAs are present not only in the mitochondria but also in the cytoplasm and nucleus, implying complex dynamics of subcellular translocation. (C) Subcellular distribution of Piwi protein in Neuro2a cells. Piwi was found in mitochondria, nucleus, and cytoplasm (thus confirming mitochondrial localization). Lamin-B, and Tom40 antibodies were used as markers for nucleus and mitochondria fractions, respectively. β-actin antibody was used for loading control. WCE (whole cell), Nu (nucleus), Mito (mitochondria), and Cyto (cytoplasm). (For interpretation of the references to color in this figure legend, the reader is referred to the web version of this article.)

tumor-promoting role for Piwi family proteins was provided by studies showing elevated Piwi expression in several human cancer types, in positive association with epigenetic anomalies, stem cell-like characteristics, poor prognosis, high grade, and a high proliferative index [6,8,9].

In summary, in extension of previous studies in germline cells, we report a finding of expression of piRNAs and Piwi proteins in cancer cell mitochondria that are closely aligned with numerous functions of that organelle in physiological homeostasis, bioenergetics, and a growing number of pathologies.

Conflict of interest

Authors declare no potential competing interests.

Acknowledgments

This work was supported by the National Cancer Center, Republic of Korea, grant (NCC-1210460 to S.N.) and the National Research Foundation, Republic of Korea, grant (2012M3A9D1054517 to E.K.L.).

Appendix A. Supplementary data

Supplementary data associated with this article can be found, in the online version, at http://dx.doi.org/10.1016/j.bbrc.2014.02.112.

References

[1] M.C. Siomi, K. Sato, D. Pezic, et al., PIWI-interacting small RNAs: the vanguard of genome defence, Nat. Rev. Mol. Cell Biol. 12 (2011) 246–258.
[2] A. Le Thomas, K.F. Toth, A.A. Aravin, To be or not to be a piRNA: genomic origin and processing of piRNAs, Genome Biol. 15 (2014) 204.
[3] N.V. Rozhkov, M. Hammell, G.J. Hannon, Multiple roles for Piwi in silencing Drosophila transposons, Genes Dev. 27 (2013) 400–412.
[4] A. Le Thomas, A.K. Rogers, A. Webster, et al., Piwi induces piRNA-guided transcriptional silencing and establishment of a repressive chromatin state, Genes Dev. 27 (2013) 390–399.
[5] H. Ishizu, H. Siomi, M.C. Siomi, Biology of PIWI-interacting RNAs: new insights into biogenesis and function inside and outside of germlines, Genes Dev. 26 (2012) 2361–2373.
[6] S. Bamezai, V.P. Rawat, C. Buske, Concise review: the Piwi–piRNA axis: pivotal beyond transposon silencing, Stem Cells 30 (2012) 2603–2611.
[7] H. Heyn, H.J. Ferreira, L. Bassas, et al., Epigenetic disruption of the PIWI pathway in human spermatogenic disorders, PLoS ONE 7 (2012) e47892.
[8] S. Siddiqi, I. Matushansky, Piwis and piwi-interacting RNAs in the epigenetics of cancer, J. Cell. Biochem. 113 (2012) 373–380.
[9] R. Suzuki, S. Honda, Y. Kirino, PIWI expression and function in cancer, Front. Genet. 3 (2012) 204.
[10] L. Sripada, D. Tomar, P. Prajapati, et al., Systematic analysis of small RNAs associated with human mitochondria by deep sequencing: detailed analysis of mitochondrial associated miRNA, PLoS ONE 7 (2012) e44873.
[11] T. Watanabe, S. Chuma, Y. Yamamoto, et al., MITOPLD is a mitochondrial protein essential for nuage formation and piRNA biogenesis in the mouse germline, Dev. Cell 20 (2011) 364–375.
[12] T.R. Mercer, S. Neph, M.E. Dinger, et al., The human mitochondrial transcriptome, Cell 146 (2011) 645–658.
[13] A. Girard, R. Sachidanandam, G.J. Hannon, et al., A germline-specific class of small RNAs binds mammalian Piwi proteins, Nature 442 (2006) 199–202.
[14] J. Goecks, A. Nekrutenko, J. Taylor, Galaxy: a comprehensive approach for supporting accessible, reproducible, and transparent computational research in the life sciences, Genome Biol. 11 (2010) R86.
[15] H. Li, R. Durbin, Fast and accurate short read alignment with Burrows–Wheeler transform, Bioinformatics 25 (2009) 1754–1760.
[16] H. Li, B. Handsaker, A. Wysoker, et al., The Sequence Alignment/Map format and SAMtools, Bioinformatics 25 (2009) 2078–2079.
[17] A.R. Quinlan, I.M. Hall, BEDTools: a flexible suite of utilities for comparing genomic features, Bioinformatics 26 (2010) 841–842.
[18] P.M. Krzyzanowski, F.D. Price, E.M. Muro, et al., Integration of expressed sequence tag data flanking predicted RNA secondary structures facilitates novel non-coding RNA discovery, PLoS ONE 6 (2011) e20561.
[19] L.R. Meyer, A.S. Zweig, A.S. Hinrichs, et al., The UCSC Genome Browser database: extensions and updates 2013, Nucleic Acids Res. 41 (2013) D64–D69.
[20] S.W. Yu, H. Wang, M.F. Poitras, et al., Mediation of poly(ADP-ribose) polymerase-1-dependent cell death by apoptosis-inducing factor, Science 297 (2002) 259–263.
[21] C.R. Galiveti, T.S. Rozhdestvensky, J. Brosius, et al., Application of housekeeping npcRNAs for quantitative expression analysis of human transcriptome by real-time PCR, RNA 16 (2010) 450–461.
[22] M.I. Sanchez, T.R. Mercer, S.M. Davies, et al., RNA processing in human mitochondria, Cell Cycle 10 (2011) 2904–2916.
[23] A. Furia, M. Moscato, G. Cali, et al., The ribonuclease/angiogenin inhibitor is also present in mitochondria and nuclei, FEBS Lett. 585 (2011) 613–617.
[24] J.T. Robinson, H. Thorvaldsdottir, W. Winckler, et al., Integrative genomics viewer, Nat. Biotechnol. 29 (2011) 24–26.
[25] J. Cheng, J.M. Guo, B.X. Xiao, et al., PiRNA, the new non-coding RNA, is aberrantly expressed in human cancer cells, Clin. Chim. Acta 412 (2011) 1621–1625.
[26] M.G. Claros, P. Vincens, Computational method to predict mitochondrially imported proteins and their targeting sequences, Eur. J. Biochem. 241 (1996) 779–786.
[27] D.M. Thompson, R. Parker, Stressing out over tRNA cleavage, Cell 138 (2009) 215–219.
[28] P.K. Padmanabhan, C. Dumas, M. Samant, et al., Novel features of a PIWI-like protein homolog in the parasitic protozoan Leishmania, PLoS ONE 7 (2012) e52612.
[29] A.H. Schapira, Mitochondrial diseases, Lancet 379 (2012) 1825–1834.
[30] M.B. Sporn, K.T. Liby, NRF2 and cancer: the good, the bad and the importance of context, Nat. Rev. Cancer 12 (2012) 564–571.
[31] A. Janic, L. Mendizabal, S. Llamazares, et al., Ectopic expression of germline genes drives malignant brain tumor growth in Drosophila, Science 330 (2010) 1824–1827.